

*Full Length Research Paper*

## **Andrographolide induces cell cycle arrest and apoptosis in PC-3 prostate cancer cells**

**Hui Chyn Wong<sup>1</sup>, Sreenivasa Rao Sagineedu<sup>1</sup>, Nordin Haji Lajis<sup>1</sup>, Seng Cheong Loke<sup>2</sup> and Johnson Stanslas<sup>1,3\*</sup>**

<sup>1</sup>Laboratory of Natural Products, Institute of Bioscience, Universiti Putra Malaysia, 43400, Serdang, Selangor, Malaysia.

<sup>2</sup>Institute of Gerontology, Faculty of Medicine and Health Sciences, Universiti Putra Malaysia, 43400, Serdang, Selangor, Malaysia.

<sup>3</sup>Pharmacotherapeutics Unit, Department of Medicine, Faculty of Medicine and Health Sciences, Universiti Putra Malaysia, 43400, Serdang, Selangor, Malaysia.

Accepted 09 August, 2018

**Andrographolide (AGP)**, the major phytoconstituent isolated from *Andrographis paniculata* was found to exhibit growth inhibition and cytotoxicity against the hormone-independent (PC-3 and DU-145) and hormone-dependent (LNCaP) prostate cancer cell lines via the microculture tetrazolium (MTT) assay. Due to its greater cytotoxic potency and selectivity towards PC-3 cells, flow cytometry was used to analyze the cell cycle distribution of control and treated PC-3 cells whereas Annexin V-FITC/PI flow cytometry analysis was carried out to confirm apoptosis induced by AGP in PC-3 cells. Cell cycle and apoptotic regulatory proteins were determined by western blot analysis. AGP was found to induce G2/M cell cycle arrest which led to predominantly apoptotic mode of cell death. Mechanistically, AGP was found to downregulate CDK1 without affecting the levels of CDK4 and cyclin D1. Induction of apoptosis was associated with an increase in activation and expression of caspase 8 which then is believed to have induced cleavage of Bid into tBid. In addition, activation and enhancement of executioner caspase 9 and Bax proteins without affecting Bcl-2 protein levels were observed.

**Key words:** Andrographolide, prostate cancer, cell cycle, cyclin-dependent kinases, apoptosis, caspase 8, caspase 9, Bcl-2 family.

### **INTRODUCTION**

Today, prostate cancer has become a major health problem, being the most frequently diagnosed noncutaneous cancer and the second-leading cause of cancer-related deaths in men worldwide (Jemal et al., 2010). Androgen-deprivation therapy is the major treatment in recurrent and metastatic prostate cancer (Ohlson et al., 2005; Mercader et al., 2007). However, in most cases, prostate cancer progresses to an apoptosis-resistant androgen-independent stage for which there is no available therapy (Navarro et al., 2002; Debes and

Tindall, 2004). It is therefore important to understand the molecular mechanisms underlying prostate cancer progression, and how prostate cancer cells evade apoptotic mechanisms that give rise to their uncontrolled growth behaviour. However, while we await more conclusive evidences of good drug targets in prostate cancer, there is a need to discover new agents that have the potential to induce growth arrest and apoptosis in metastatic prostate cancer cells.

Andrographolide (AGP) is a natural compound isolated from *Andrographis paniculata*. It is bestowed with an interesting pharmacophore that displays various pharmacological activities including anticancer activity (Stanslas et al., 2001; Rajagopal et al., 2003; Jada et al., 2007; Manikam and Stanslas, 2009). Recent findings

\*Corresponding author. E-mail: rcxs@medic.upm.edu.my, jstanls@yahoo.co.uk. Tel: +603 89472310. Fax: +603 89472759.

suggest AGP could induce apoptosis by activating the caspase cascade and regulating Bcl-2 family proteins in human tumour cells (Zhou et al., 2006; Kim et al., 2005). In the human leukaemic HL-60 cells, induction of apoptosis was linked with leakage of mitochondrial cytochrome *c* and upregulation of Bax expression (Cheung et al., 2005). The compound also displayed cell differentiation and apoptosis in promyelocytic-leukaemia cells (Manikam and Stanslas, 2009).

The elucidation of the mechanism of action of AGP remains inexplicable as many models have been proposed to illustrate the antitumour properties of AGP (Zhou et al., 2006). However, the most intriguing finding by Liang et al. (2008) revealed that this compound has a novel mechanism through its ability to promote degradation of the oncogene v-Src through attenuation of the Erk1/2 signalling pathway. A most recent finding by Tan et al. (2010) points to AGP's ability to exert its antitumour activity by affecting the receptor trafficking in cancer cells. Previously, Kim et al. (2005) reported the compound induced apoptosis in PC-3 cells by activating caspase-3 and -8. Hence, the involvement of an extrinsic caspase cascade for induction of apoptosis was proposed. However, the exact mechanism of anti-prostate cancer activity of AGP is still largely unknown. In the present investigation, we first evaluated cytotoxicity of AGP in 3 different cell lines (hormone-independent – PC-3 and DU-145, and hormone-dependent – LNCap) with different molecular characteristics to determine if the compound exerts selective killing of the cancer cells (Belldegrun et al., 2000). We found the PC-3 cells to be exquisitely sensitive. As such, the molecular mechanisms of cell cycle arrest and apoptosis were studied in this cell line.

## MATERIALS AND METHODS

### Chemicals and reagents

AGP was isolated in-house from *A. paniculata* according to a method reported previously (Jada et al., 2006). RPMI 1640 medium with L-glutamine, penicillin-streptomycin and trypsin-EDTA were purchased from GIBCO (Auckland, New Zealand). Tissue culture flasks and 96-well flat-bottomed plates were obtained from TPP (Trasadingen, Switzerland). Foetal bovine serum (FBS), phosphate buffered saline (PBS) tablets, Triton X-100, Tris-base, Tris-HCl, propidium iodide (PI) and RNase A were purchased from Sigma (St. Louis, USA). MTT was obtained from PhytoTechnology Laboratories (Kansas, USA). Ammonium persulphate was purchased from BDH Chemicals Ltd (Poole, UK). SDS,  $\beta$ -mercaptoethanol, TEMED, glycerol and Tween 20 were obtained from Merck (Hohenbrunn, Germany). DMSO was purchased from Fisher Scientific (Leicestershire, UK). EDTA, glycine and Bio-Rad protein assay reagent were obtained from Bio-Rad Laboratories Inc. (California, USA). Bromophenol blue, acrylamide PAGE, methylenebisacrylamide were purchased from Amersham Biosciences (Uppsala, Sweden) and ECL plus Western blotting reagent pack and ECL plus Western detection system were obtained from Amersham Biosciences (Buckinghamshire, UK). Protease inhibitor cocktail set III was supplied by Calbiochem

(California, USA). BenchMark<sup>TM</sup> Prestained protein ladder was purchased from Invitrogen (California, USA). NitroBind (Pure Nitrocellulose Membrane, 0.45  $\mu$ M) was obtained from Osmonic Inc. (California, USA). Monoclonal anti- $\beta$ -actin (clone AC-74) was purchased from Sigma (St. Louis, USA). Annexin V-FITC apoptosis detection kit, mouse monoclonal antibodies against caspase 8 and, Bid were obtained from BD Biosciences (California, USA) and Cell Signalling Technology, Inc. (Massachusetts, USA), respectively. Mouse monoclonal antibodies against caspase 9, Bcl-2, Bax, CDK4, CDK1 and cyclin D1 were purchased from Calbiochem (California, USA).

### Cell lines and cell culture

Human prostate cancer cell lines PC-3, DU-145 (androgen-independent) and LNCaP (androgen-dependent) were purchased from ATCC (Manassas, VA, USA). The cell lines were maintained in RPMI-1640 medium with L-glutamine, supplemented with 10% heat inactivated (56°C for 1 h) FBS at 37°C in an atmosphere of 5% CO<sub>2</sub> and 95% air.

### MTT cell viability assay

The assay was carried out based on the method described by Mosmann (1983). Briefly, cells were plated in 96-well flat-bottomed tissue culture plates with 3000 cells per well in 180  $\mu$ l culture media. This was followed by incubation at 37°C (5% CO<sub>2</sub> and 95% air) overnight to allow cell attachment onto the wells. A stock concentration of 100 mM for each test agent was made up in DMSO. The working concentrations ranging from 1 to 1000  $\mu$ M were obtained by serial dilution of stock in culture medium and 20  $\mu$ l of each of the concentration was added into the appropriate wells in four replicates to obtain final concentrations ranging from 0.1 to 100  $\mu$ M. The control cells were treated with the highest concentration of DMSO (0.1%) as vehicle control. Following a further 96 h incubation, 50  $\mu$ l MTT (2 mg/ml in PBS) was added per well and the plates were incubated for 4 h to allow metabolism of MTT by cellular mitochondrial dehydrogenases. The excess MTT was aspirated and the formazan crystals formed were dissolved by the addition of 100  $\mu$ l of DMSO. The absorbance of purple formazan which is proportional to the number of viable cells was read at 550 nm using VersaMax microplate reader (Molecular Devices, California, USA). The results were analysed using SoftMaxPro software. Using 0 and 96 h MTT absorbance values, the semi-log dose-response growth curves (percentage of growth versus concentration) were constructed, from which the GI<sub>50</sub> (concentration that produces 50% growth inhibition), TGI (concentration that produces total growth inhibition or cytostatic effect and LC<sub>50</sub> (-50% growth: lethal concentration or 'net cell killing' or cytotoxicity parameter) were determined (Jada et al., 2008).

### Cell cycle analysis

Control and treated floating and adherent cells were collected by trypsinization and pelleted at 100 g for 10 min. Cells were washed two times with cold 1% BSA-PBS buffer. Upon centrifugation, the resulting cell pellet was dislodged before fixing the single cells in 70% ice-cold ethanol, followed by incubation for 15 min on ice. The fixed cells were stored at -20°C until flow cytometry analysis. On the day of analysis, the cells in ethanol were centrifuged at 100 g for 10 min. Cells were washed twice in 1% BSA-PBS buffer and resuspended in 1 ml PBS before being transferred to a polystyrene round bottom tube (12 × 75 mm) (BD Biosciences, California, USA). Twenty microlitre of 10 mg/ml RNase A and 40  $\mu$ l of 2.5 mg/ml PI

**Table 1.** GI<sub>50</sub>, TGI and LC<sub>50</sub> values of AGP at 24, 48, 72 and 96 h time points in PC-3, DU-145 and LNCaP prostate cancer cells.

Time (h)	GI <sub>50</sub> (μM)				TGI (μM)				LC <sub>50</sub> (μM)		
	PC-3 <sup>#</sup>	DU-145	LNCaP	PC-3 <sup>#</sup>	DU-145	LNCaP	PC-3 <sup>#</sup>	DU-145	LNCaP	DU-145	LNCaP
24*	1.5 ± 0.5	6.4 ± 1.4	8.8 ± 1.0	4.5 ± 1.0	10.2 ± 1.4	11.5 ± 1.0	14.1 ± 1.4	25.1 ± 1.3	24.7 ± 1.2		
48	6.3 ± 1.2	7.0 ± 1.2	10.4 ± 1.3	14.9 ± 1.3	16.3 ± 1.2	20.4 ± 1.2	23.3 ± 1.0	25.3 ± 0.9	35.2 ± 1.4		
72	6.4 ± 1.3	12.6 ± 1.6	19.8 ± 1.5	18.3 ± 1.6	19.4 ± 1.9	31.5 ± 1.2	29.4 ± 1.9	29.1 ± 1.5	44.2 ± 1.2		
96	9.7 ± 1.3	18.7 ± 1.0	34.2 ± 1.0	19.9 ± 1.0	29.7 ± 1.7	55.0 ± 1.0	31.6 ± 1.2	41.7 ± 1.1	72.9 ± 1.0		

\*Statistically significant ( $p < 0.05$ ) compared with 48, 72 or 96 h time points. <sup>#</sup>Statistically significant ( $p < 0.05$ ) compared with DU-145 or LNCaP cells except for TGI (72 h) and LC<sub>50</sub> (48 and 72 h) of DU-145. The cells were treated for 24-, 48-, 72- and 96 h with at least four different concentrations of compounds ranging from 0.1 to 100 μM. MTT assay was used to calculate the GI<sub>50</sub>, TGI and LC<sub>50</sub> values (expressed in μM). Values represent mean ± SD of three independent experiments.

were added and the tubes were incubated at 37°C for 30 min. The DNA content of 10,000 cells for each determination was measured using FACSCALIBUR flow cytometer (Becton Dickinson, Sunnyvale, California) in which an argon laser (488 nm) was used to excite PI and emission above 550 nm was collected (Jada et al., 2008; Ormerod, 1999). The single cell population was gated and DNA histograms were generated using WinMDI 2.8 (Joseph Trotter, The Scripps Research Institute, <http://facs.scripps.edu>) flow cytometry programme. For quantitation of percentage of cells in various phases, Cyclched<sup>TM</sup> (Terry Hoy, University of Wales, College of Medicine (UWCM) flow cytometry software was used.

#### Annexin V-FITC staining analysis by flow cytometry

Floating and trypsinized adherent cells were collected by centrifugation at 100 g for 10 min. The cells were washed twice with ice-cold PBS. Upon centrifugation, the resulting cell pellet was resuspended in 1X annexin V Binding Buffer (1 part of 10X annexin V binding buffer and 9 parts distilled water) at a concentration of 1 × 10<sup>6</sup> cells/mL and 100 μL of the solution (1 × 10<sup>5</sup> cells) was transferred to a 5 ml polystyrene round bottom tube (12 × 75 mm) (BD Biosciences, California, USA). Five microliter of annexin V-FITC and 5 μL of PI were added to the tube and the sample was mixed gently. Following 15 min incubation at room temperature (25°C) in the dark, 400 μL of 1X annexin V binding buffer was then added into the tube and the samples were analysed immediately using FACSCALIBUR flow cytometer (Becton Dickinson, Sunnyvale, California). The green fluorescence (FITC) and red fluorescence (PI) were detected by filtration through 530 and 588 nm band pass filters, respectively. For each sample, 10,000 events were collected and the results were evaluated using WinMDI 2.8 flow cytometry software (Joseph Trotter, The Scripps Research Institute, <http://facs.scripps.edu>).

#### Western blot analysis

Exponentially growing (60% confluence) control untreated and treated cells were trypsinised, diluted in PBS, syringed and then pelleted by centrifugation at 100 g for 5 min. The cell pellet was then resuspended in lysis buffer (10 mM Tris-HCl, 1.92 mM MgCl<sub>2</sub>, 1 mM EDTA, 50 mM NaCl, 6 mM β-mercaptoethanol, 2% Triton X-100) containing 1% protease inhibitor cocktail set III (with AEBSF) and sonicated (PowerSonic 410) for 10 min on ice. The cell lysate was centrifuged at 13000 g for 10 min and the supernatant was collected and stored at -80°C in 50 μL aliquots or used immediately. The concentration of protein was determined using Bio-Rad protein assay reagent according to the manufacturer's instructions. An equal amount of protein (30 μg) per sample was separated by 10%

SDS-PAGE. After electrophoresis, the proteins were transferred to nitrocellulose membrane, blocked overnight with 5% non-fat dried milk in PBS-T at 2-8°C, reacted with mouse monoclonal primary antibodies against caspase 8 (1:2000), Bid (1:2000), caspase 9 (1:2000), Bcl-2 (1:2000), Bax (1:2000), CDK4 (1:2000), CDK1 (1:2000), cyclin D1 (1:2000) or monoclonal anti-β-actin (clone AC-74) (1:5000) and washed. After reaction with horseradish peroxidise-conjugated goat anti-mouse antibody, the immune complexes were visualized by using the chemiluminescence ECL PLUS detection reagents following the manufacturer's procedure. The reacted membrane was exposed to a chemiluminescence detector (CHEMI-SMART-3126 WL/26MX machine, Vilberlourmat, Marne la Vallee, France) and images of bands of interest were analysed using Chemi-Capt 3000 and Image J software.

#### Statistical analysis

The data are represented as mean ± SD. SPSS version 17 was utilised for analysis. Statistical comparisons were made using two-way ANOVA, after which Bonferroni and Tukey post-hoc tests were performed for comparison between individual groups. A value of  $p < 0.05$  was considered to be significant.

## RESULTS AND DISCUSSION

#### In vitro growth inhibitory properties of AGP in PC-3, DU-145 and LNCaP cells

The conventional tetrazolium-based assay was performed to calculate the GI<sub>50</sub>, TGI and LC<sub>50</sub> dose-response growth inhibitory parameters over 24 to 96 h time period in PC-3, DU-145 and LNCaP cells (Table 1). For almost all growth inhibitory parameters (GI<sub>50</sub>, TGI and LC<sub>50</sub>), PC-3 cells exhibited lowest values compared with DU-145 and LNCaP cells, at nearly all the time points. The highest activity was observed at 24 h time point, whereby a GI<sub>50</sub> of 1.5 μM was obtained. It is interesting to note that with increasing exposure time from 48 to 96 h, the values of the growth inhibitory parameters of AGP increased for all the cell lines. LNCaP cells were most resistant to growth inhibition by AGP. The differential sensitivity of the cell lines to AGP could be explained in part due to the difference in molecular characteristics of the three different prostate

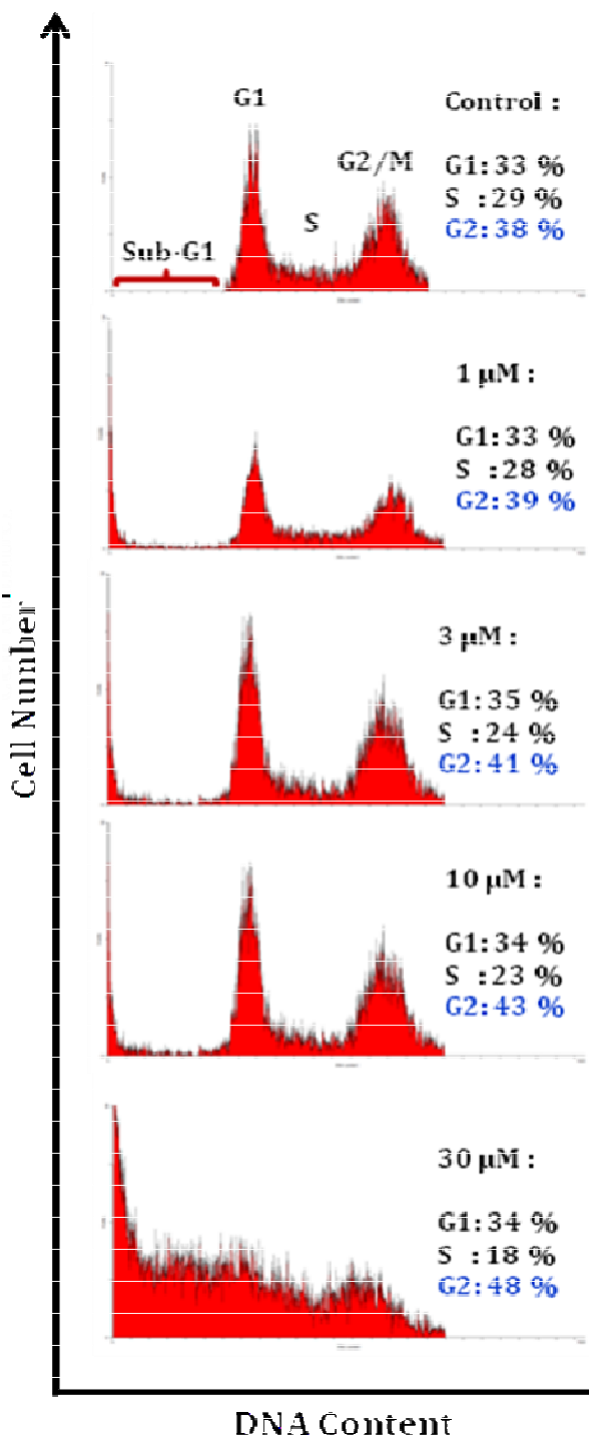


**Figure 1.** DNA histograms showing the cell cycle phase distribution of control and AGP-treated PC-3 cells at 24 h time point. These figures are from representative experiments carried out three times. The x and y axis represent DNA content and cell number, respectively. Numbers highlighted in bold correspond to the significant variations compared to control.

cancer cell lines. PC-3 and DU145 cell lines which were most sensitive to AGP are androgen-independent

whereas LNCaP cell line that was most resistant to AGP is androgen-dependent. Interestingly, both PC-3 and LNCaP cells express prostate specific antigen (PSA), and are p53-deficient and p53-wildtype, respectively. DU-145 cells on the other hand are p53-mutant. From these analyses, it is apparent that cells (PC-3) without p53-deficient, express PSA and androgen-independence are most sensitive to growth inhibition by AGP. However, LNCaP cells with hormone-dependence and p53-wildtype confer resistance to AGP. Factors other than as mentioned above may also contribute to the activity of AGP but remain inconclusive and warrants further investigations.

### Inhibition of cell cycle progression

Since AGP displayed greater cytotoxic selectivity towards PC-3 cells, flow cytometric analysis was used to measure the DNA contents of control and AGP-treated PC-3 cells to determine the cell cycle perturbations induced by the compound. Any changes in the cell cycle progression will be reflected in the appearance of the DNA histogram produced. Following exposure time of 24 h, AGP induced a G2/M phase cell cycle arrest in PC-3 cells (Figure 1). Treatment with 1, 3, 10 and 30  $\mu\text{M}$  concentrations for 24 h caused accumulation of cells in G2/M phase with a concomitant decrease of both G1 and S phase in PC-3 cells. It is noteworthy that increasing the concentration of the compound also promoted appearance of a sub-G1 population indicative of apoptotic cells.

### Effect on the cell cycle regulatory proteins in PC-3 cells treated with AGP

The CDK family of serine/threonine kinases are important regulators in the mammalian cell division cycle. The CDKs activity depends on their association with cyclins. Whilst the expression of the CDK subunit is generally constant throughout the cell cycle, the expression of each cyclin tends to be cell cycle dependent so that a specific CDK will have full activity when its cyclin partner is expressed (Morgan, 1997).

During the G1 phase, the initiation of CDK4 and CDK6 acts in association with one of three closely related cyclin subunits, D1, D2 and D3. This allows the expression of cyclin E which in turn binds to CDK2 to form a complex that allows the cell to progress from G1 into S phase (Harbour et al., 1998). As cells progress into S phase, cyclin A is expressed and becomes the primary cyclin associated with CDK2. Progression from G2 into mitosis requires the activity of the CDK, Cdc2, also known as CDK1, complexation with cyclin B, which has been shown to phosphorylate proteins regulated during mitosis (Kariya et al., 2000; Heix et al., 1998; Lane et al., 1995).

From our investigation of the cell cycle analysis, it was shown that AGP induced a G2/M phase block in PC-3

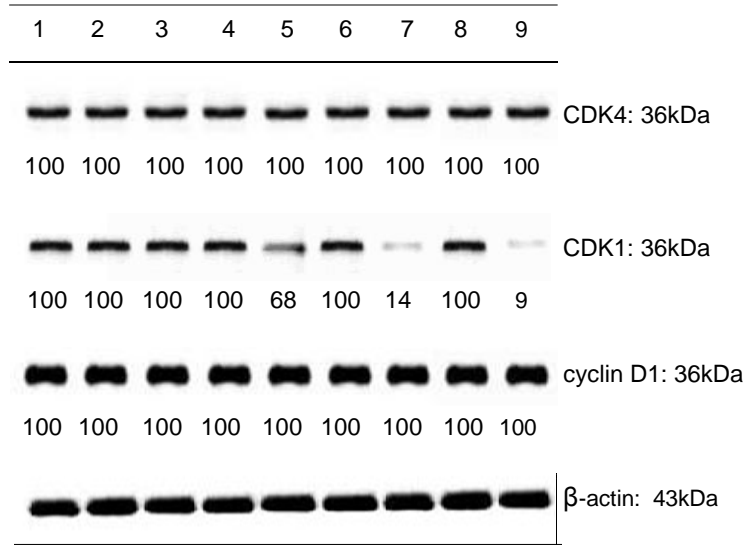


**Figure 2.** Western blot analysis of lysates of AGP-treated PC-3 cells. PC-3 cells treated with AGP for 24 h with CDK4, CDK1, cyclin D1 and  $\beta$ -actin were detected. The  $\beta$ -actin was used to ensure equal amount of protein was loaded. Lane 1: Control cells, treated medium alone without vehicle, Lane 2, 4, 6 and 8: Cells treated with DMSO in medium as vehicle, correspond to amount of DMSO in 1, 3, 10 and 30  $\mu$ M AGP respectively. Lane 3, 5, 7 and 9: Cells treated with 1, 3, 10 and 30  $\mu$ M AGP, respectively.

cells. To correlate this effect with the expression of proteins that control cell cycle progression namely CDK1 (G2/M phase), CDK4 and cyclin D1 (G1 phase), western blots were performed on protein lysates of PC-3 cells treated with AGP for 24 h (Figure 2). AGP-treated cells displayed down-regulation of CDK1 expression in a concentration-dependent fashion without alterations to the CDK4 and cyclin D1 expression. Therefore, these results strongly suggest that the G2/M phase cellcycle arrest occurred in PC-3 cells was most likely due to the down-regulation of CDK1 expression.

#### Annexin V-FITC flow cytometry analysis of apoptosis in AGP-treated PC-3 cells

It was noted that the DNA histograms used for cell cycle analysis consistently showed the presence of apoptotic populations among cells treated with AGP. To ascertain that the mode of cell death was by apoptosis, annexin V-FITC flow cytometry analysis was carried out. Apoptosis is characterised by distinct biochemical features, in which activation of catabolic processes and enzymes occurs before cytolysis, thereby facilitating cell morphological changes, such as phosphatidylserine (PS) externalisation to the cell surface, mitochondrial alterations, membrane blebbing, cell shrinkage and nuclear condensation/fragmentation (Herngartner, 2000; Hotz et al., 1994). Early apoptotic cells tend to exhibit PS on outer cell membrane,

which is normally positioned across the inner membrane (Fadok et al., 1992) and it has a strong binding affinity to annexin V (Vermes et al., 2000). Early and late apoptotic cells have been thus known to be quantified by flow cytometry using annexin V-FITC and DNA-binding fluorochrome PI (Andree et al., 1990). Determination of exposure of PS on the cell surface as an early event in PC-3 cells treated with AGP at 24 h time point was confirmed by annexin V-FITC (Figure 3). The percentage of viable cells (J1) in AGP-treated PC-3 cells compared to control cells decreased in a concentration-dependent fashion at 24 h with a concurrent increase in the percentage of apoptotic cells (early apoptotic (J2) and late apoptotic (J3)). Treatment with 10  $\mu$ M concentration induced nearly 86% of the cells to undergo early and late apoptosis. Additionally, exposure of cells to high concentration of AGP at 30  $\mu$ M induced necrotic cells (J4). These results confirm that apoptosis is the main mode of cell death induced by AGP in PC-3 cells.

#### Effect on the apoptotic regulatory proteins in PC-3 cells treated with AGP

The apoptotic signalling pathways are divided into extrinsic and intrinsic pathways. The extrinsic pathway originates in the cell exterior and involves cell surface receptors that belong to the TNF receptor (TNF-R) family, which trimerize and recruit adaptor proteins on ligand

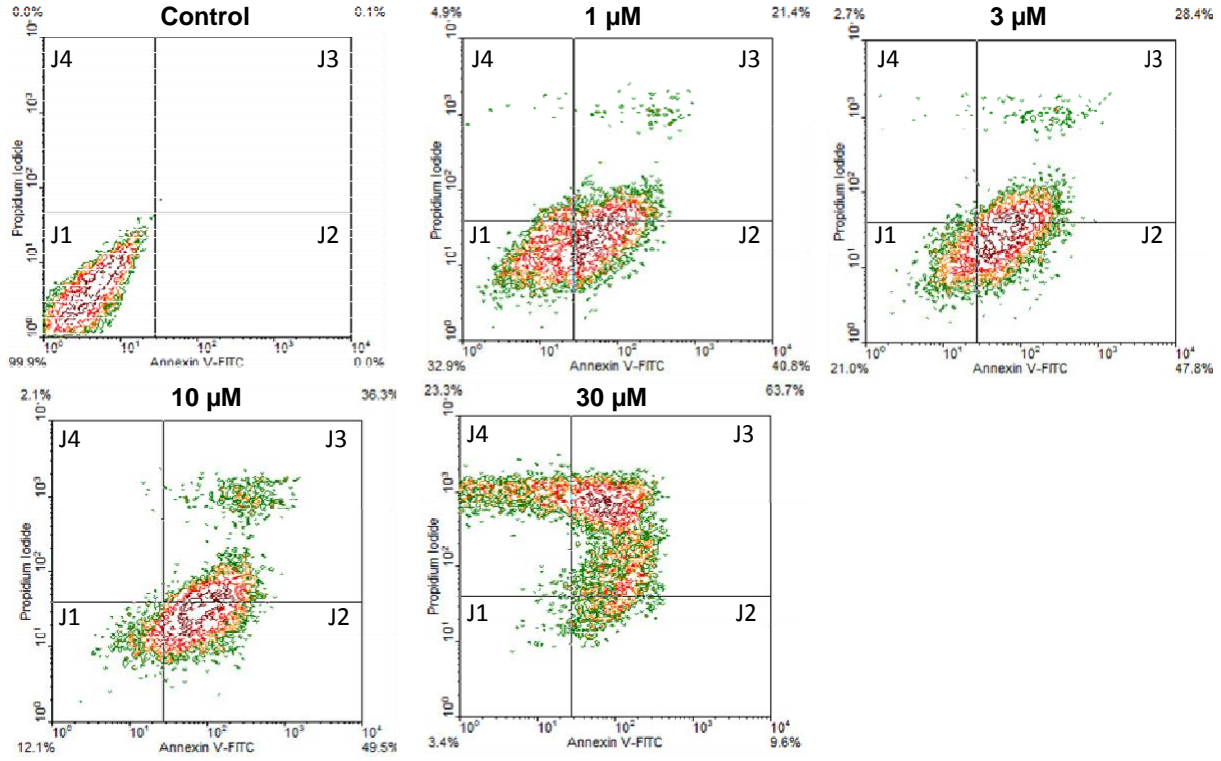


**Figure 3.** Contour plots showing the percentage distribution of control and AGP (1, 3, 10 and 30  $\mu$ M) treated PC-3 cells at 24 h time point. Quadrants: J1: Viable cells, J2: Early apoptotic cells, J3: Late-apoptotic cells, J4: Necrotic cells.

binding. The adaptor proteins recruit pro-caspase-8, thus forming the death-inducing signalling complex (DISC). The local concentration of several pro-caspase-8 molecules leads to their autocatalytic activation and release of active caspase-8 that processes downstream effector caspases, which subsequently cleave specific substrates resulting in cell death (Hengartner, 2000; Strasser et al., 2000; Fulda and Debatin, 2006). The intrinsic pathway is activated in response to cell-death signals originating from the cell interior and is mediated by members of the Bcl-2 family, leading to the release of cytochrome c from the mitochondria. In the cytosol, cytochrome c and the adaptor protein Apaf-1 form the apoptosome that activates caspase-9, which in turn activates the caspase cascade. The activation of the caspase cascade can be blocked by inhibitors of apoptosis proteins (IAPs), which can be upregulated in response to survival signals (Hengartner, 2000; Strasser et al., 2000; Fulda and Debatin, 2006). Cross talk between the extrinsic and intrinsic pathways is mediated by Bid, a proapoptotic Bcl-2 family member. Caspase-8 mediated cleavage of Bid increases its activity and results in translocation to the mitochondria, where it acts in concert with two other proapoptotic proteins, Bax and Bak, to induce cytochrome c release, thereby activating the intrinsic pathway (Hengartner, 2000; Strasser et al., 2000).

The involvement of caspase 8 as an initiator caspase

and caspase 9 as an executioner caspase were studied. Western blots were performed on protein lysates of PC-3 cells treated with 1, 3, 10 and 30  $\mu$ M of AGP for 24 h (Figure 4). A dose-dependent increase in expression and activation of caspase 8 was observed with increasing concentrations of AGP at 24 h. Similarly for caspase 9, the caspase 9 (35 kDa) underwent overwhelming activation to cleaved activated form (10 kDa) in a concentration-dependent manner. We then looked at proapoptotic proteins Bid and Bax, Bid was found to be involved also by displaying a dose-dependent activation into tBid, which provides a critical step cross-linking the extrinsic cell death receptor signalling pathway to mitochondria upon caspase 8-mediated cleavage. It has also been well established that caspase 8-mediated Bid cleavage and subsequent Bid mitochondrial translocation mediate mitochondria alteration in response to activation of cell surface death receptor (Luo et al., 1998; Li et al., 1998). One of the key molecules activated in response to Bid cleavage and mitochondrial translocation is Bax, whereby it undergoes transformation and oligomerization to form pores in the outer mitochondrial membrane, leading to the release of pro-apoptotic proteins from mitochondria, such as cytochrome c (Kuwana et al., 2005; Cory and Adams, 2002). Bax has been considered as one of the most important pro-apoptotic Bcl-2 members promoting mitochondrial apoptotic pathway (Kuwana et al., 2005). Furthermore, it is known that Bax's

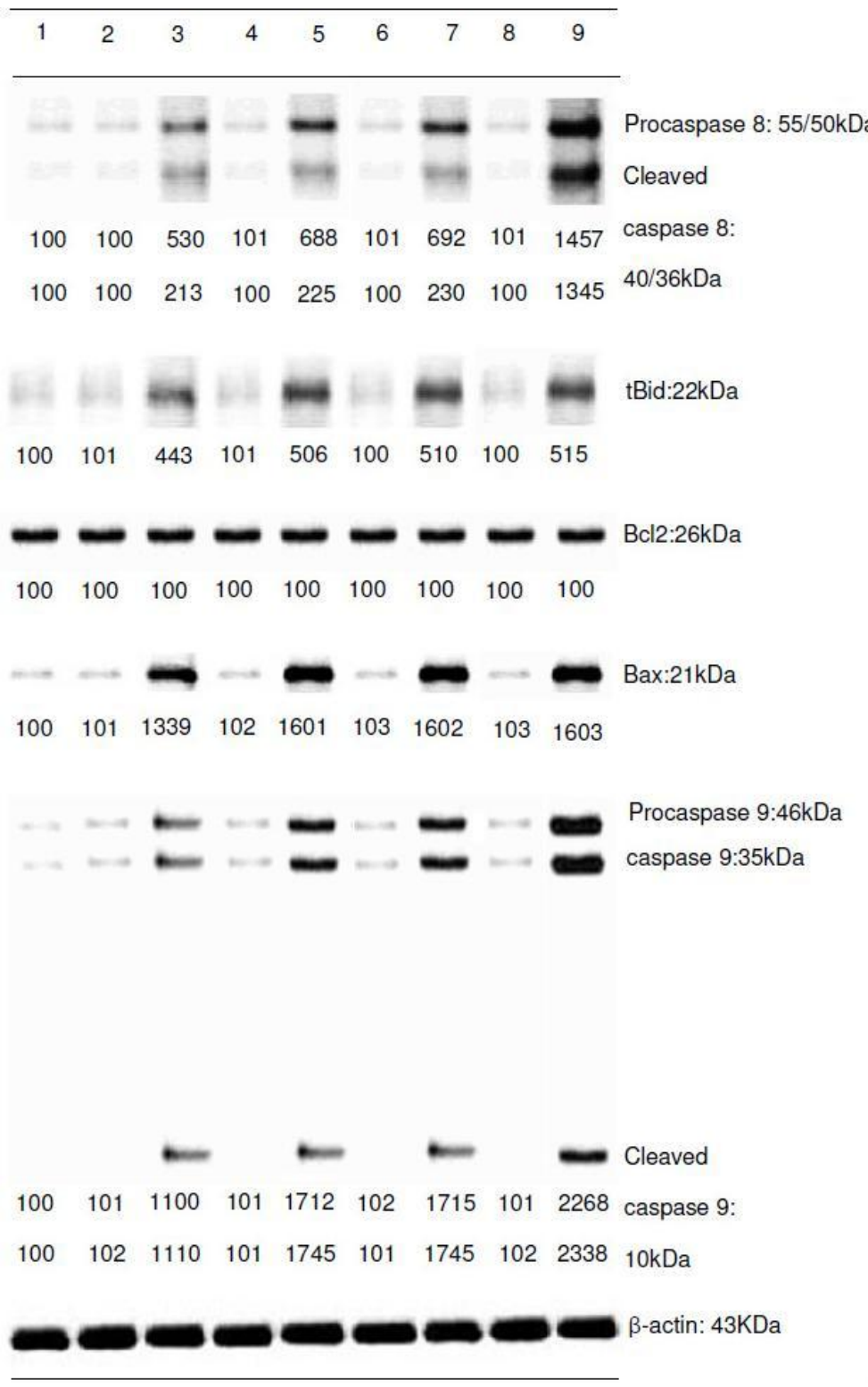


**Figure 4.** Western blot analysis of lysates of AGP-treated PC-3 cells. PC-3 cells treated with AGP for 24 h with caspase 8, Bid, caspase 9, Bcl-2, Bax and  $\beta$ -actin were detected. The  $\beta$ -actin was used to ensure equal amount of protein were loaded. Lane 1: Control cells, treated medium alone without vehicle, Lane 2, 4, 6 and 8: Cells treated with DMSO in medium as vehicle, correspond to amount of DMSO in 1, 3, 10 and 30  $\mu$ M AGP respectively. Lane 3, 5, 7 and 9: Cells treated with 1, 3, 10 and 30  $\mu$ M AGP, respectively.

proapoptotic activity is subject to the regulation by other Bcl-2 family members. For instance, the anti-apoptotic Bcl-2 protein is able to block apoptosis by binding to Bax to form Bcl-2–Bax heterodimers (Yi et al., 2003).

Our investigation revealed increasing concentration of AGP treatment enhanced Bax protein activation without altering the expression of Bcl-2 protein. It is thus believed increase in pro-apoptotic function of Bid and Bax led to efficient apoptosis in PC-3 cells. Although our data clearly suggested that Bid is a critical upstream regulator of the pro-apoptotic function of Bax, activation and translocation of Bax also can be initiated by other mechanisms, such as direct activation by Bim (Kuwana et al., 2005) and enhanced expression induced by tumor suppressor p53 (Hanahan and Weinberg, 2000; Liu et al., 2004). Therefore, these observations strongly support the notion that Bcl-2 family members especially the proapoptotic proteins are critical regulators in AGP-induced apoptosis. From these observations, we propose, AGP induced apoptotic cell death by the death receptor pathway, which then led to activation of initiator caspases 8 followed by activation of bid and bax in mitochondria that in turn facilitated the release of apoptotic factors and thus amplified the caspase cascade (executioner caspase 9). In summary, data from this study provide convincing evidence that the pro-apoptotic Bcl-2 family members, Bid and Bax are the key mediators in relaying the cell death signalling initiated by AGP from caspase 8 to mitochondria eventually leading to apoptotic cell death. This was further supported by a study by Kim et al. (2005) who proposed that AGP-treated PC-3 cells underwent apoptosis through activation of the extrinsic caspase cascade via activation of caspase 8 and later by Zhou et al. (2006) whereby they found that AGP induced apoptosis in human cancer cells (hepatoma cancer cell HepG2, human cervical cancer cell HeLa and human breast cancer cell MDA-MB-231), via activation of the caspase 8-dependent Bid cleavage, followed by a series of sequential events including Bax conformational change and mitochondrial translocation, cytochrome c release from mitochondria, and activation of caspase 9 and 3. Taken together, the pro-apoptotic Bcl-2 family members (Bid and Bax) are the key mediators in relaying the cell death signalling initiated by AGP from caspase 8 to mitochondria and then to downstream effector caspases and eventually leading to apoptotic cell death.

## Conclusion

Data obtained from this study form a basis to conclude that AGP displayed selective inhibitory properties through induction of G2/M phase cell cycle arrest and apoptosis in PC-3 prostate cancer cells compared with DU-145 and LNCaP cells. Although understanding the exact molecular mechanisms underlying AGP-induced cell cycle arrest and apoptosis in prostate cancer cells is far from conclusive, this present study provided new insights

for further investigation into the molecular mechanism of anti-prostate cancer activity by AGP.

## ACKNOWLEDGEMENTS

The Ministry of Higher Education is thanked for funding this project through the RUGS grant scheme (04-01-09-0713RU). Hui Chyn Wong is a recipient of the National Science Fellowship (NSF) awarded by the Ministry of Science, Technology and Innovation of Malaysia (MOSTI). We are grateful to Mr. Lim Siang Hui from Cancer Research Initiatives Foundation (CARIF), Malaysia, for assistance in the flow cytometry work.

## REFERENCES

- Andree HA, Reutelingsperger CP, Hauptmann R, Hemker HC, Hermens WT, Willems GM (1990). Binding of vascular anticoagulation alpha (VAC alpha) to planar phospholipid bilayer. *J. Biol. Chem.*, 265: 4923-4928.
- Belldegrun A, Kirby RS, Newling DWW (2000). New Perspectives in Prostate Cancer, Second Edition. Isis Medical Media, Maryland, USA, 91-104.
- Cheung HY, Cheung SH, Li J, Cheung CS, Lai WP, Fong WF (2005). Andrographolide isolated from *Andrographis paniculata* induces cell cycle arrest and mitochondrial-mediated apoptosis in human leukemic HL-60 cells. *Planta. Med.* 71: 1106-1111.
- Cory S, Adams JM (2002). The Bcl2 family: regulators of the cellular life-or-death switch. *Nat. Rev. Cancer.*, 2: 647-656.
- Debes JD, Tindall DJ (2004). Mechanisms of androgen-refractory prostate cancer. *N. Engl. J. Med.*, 351: 1488-1490.
- Fadok VA, Voelker DR, Campbell PA, Cohen J, Bratton DL, Henson PM (1992). Exposure of phosphatidylserine on the surface of apoptotic lymphocytes triggers specific recognition and removal by macrophages. *J. Immunol.*, 148: 2207-2216.
- Fulda S, Debatin KM (2006). Extrinsic versus intrinsic apoptosis pathways in anticancer chemotherapy. *Oncogene.* 25: 4798-4811.
- Hanahan D, Weinberg RA (2000). The hallmarks of cancer. *Cell.* 100: 57-70.
- Harbour JW, Luo RX, Dei Santi A, Postigo AA, Dean DC (1998). CDK phosphorylation triggers sequential intramolecular interactions that progressively block Rb functions as cell move through G1. *Cell.* 98: 859-869.
- Heix J, Vene A, Voit R, Budde A, Michaelidis TM, Gummt I (1998). Mitotic silencing of human rRNA synthesis: inactivation of the promoter selectivity factor SL1 by cdc2/cyclin B-mediated phosphorylation. *EMBO. J.*, 17: 7373-7381.
- Hengartner MO (2000). The biochemistry of apoptosis. *Nature.* 407: 770-776.
- Hotz MA, Gong J, Traganos F, Darzynkiewicz Z (1994). Flow cytometric detection of apoptosis: comparisons of the assays of *in situ* DNA degradation and chromatin changes. *Cytometry.* 15: 237-244.
- Jada SR, Hamzah AS, Lajis NH, Saad MS, Stevens MFG, Stanslas J (2006). Semisynthesis and cytotoxic activities of andrographolide analogues. *J. Enzyme Inhib. Med. Chem.*, 21: 145-155.
- Jada SR, Subur GS, Matthews C, Hamzah AS, Lajis NH, Saad MS, Stevens MF, Stanslas J (2007). Semisynthesis and *in vitro* anticancer activities of andrographolide analogues. *Phytochemistry.* 68: 904-912.
- Jada SR, Matthews C, Saad MS, Hamzah AS, Lajis NH, Stevens

- MFG, Stanslas J (2008). Benzylidene derivatives of andrographolide inhibit growth of breast and colon cancer cell *in vitro* by inducing G1 cell cycle arrest and apoptosis. Br. J. Pharmacol., 155: 641-654.
- Jemal A, Siegel R, Xu J, Ward E (2010). Cancer Statistics. CA Cancer J. Clin., 60: 277-300.
- Kariya K, Koyama S, Nakashima S, Oshiro T, Morinaka K, Kikuchi A (2000). Regulation of complex formation of POB1/epsin /adaptor protein complex 2 by mitotic phosphorylation cdc2/cyclin B-mediated phosphorylation. J. Biol. Chem., 275: 18399-18406.
- Kim TG, Hwi KK, Hung CS (2005). Morphological and biochemical changes of andrographolide-induced cell death in human prostatic adenocarcinoma PC-3 cells. *In Vivo*. 19: 551-557.
- Kuwana T, Bouchier-Hayes L, Chipuk JE, Bonzon C, Sullivan BA, Green DR (2005). BH3 domains of BH3-only proteins differentially regulate Bax-mediated mitochondrial membrane permeabilization both directly and indirectly. Mol. Cell., 17: 525-535.
- Lane HA, d'Herin P, Harper M, Kress M, Nigg EA (1995). Phosphorylation by p34cdc2 regulates spindle association of human Eg5, a kinesin-related motor essential for bipolar spindle formation *in vivo*. Cell. 83: 1159-1169.
- Li H, Zhu H, Xu CJ, Yuan J (1998). Cleavage of BID by caspase 8 mediates the mitochondrial damage in the Fas pathway of apoptosis. Cell. 94: 491-501.
- Liang FP, Lin CH, Kuo CD, Chao HP, Fu SL (2008). Suppression of v-Src transformation by andrographolide via degradation of the v-Src protein and attenuation of the Erk signalling pathway. J. Biol. Chem. 283: 5023-5033.
- Liu FT, Goff LK, Hao JH, Newland AC, Jia L (2004). Increase in the ratio of mitochondrial Bax/Bcl-XL induces Bax activation in human leukemic K562 cell line. Apoptosis. 9: 377-384.
- Luo X, Budihardjo I, Zou H, Slaughter C, Wang X (1998). Bid a Bcl-2 interacting protein, mediates cytochrome c release from mitochondria in response to activation of cell surface death receptors. Cell. 94: 481-490.
- Manikam SD, Stanslas J (2009). Andrographolide inhibits growth of promyelocytic leukemia cells by inducing retinoic acid receptor-independent cell differentiation and apoptosis. J. Pharm. Pharmacol. 61: 78-79.
- Mercader M, Sengupta S, Bodner BK, Manecke RG, Cosar EF, Moser MT, Ballman KV, Wojcik EM, Kwon ED (2007). Early effects of pharmacological androgen deprivation in human prostate cancer. BJU Int., 99: 60-67.
- Morgan DO (1997). Cyclin-dependent kinases: engines, clocks, and microprocessors. Annu. Rev. Cell Dev. Biol., 13: 261-291.
- Mosmann T (1983). Rapid colorimetric assay for cellular growth and survival: application to proliferation and cytotoxicity assays. J. Immunol. Meth., 65: 55-63.
- Navarro D, Luzardo OP, Fernandex L, Chesa N, Diaz-Chico BN (2002). Transition to androgen-independence in prostate cancer. J. Steroid Biochem. Mol. Biol., 81: 191-201.
- Ohlson N, Wikstrom P, Stattin P, Bergh A (2005). Cell proliferation and apoptosis in prostate tumors and adjacent non-malignant prostate tissue in patients at different time points after castration treatment. Prostate. 62: 307-315.
- Ormerod MG (1999). Flow Cytometry: A Practical Approach. Oxford University Press, New York.
- Rajagopal S, Kumar RA, Deevi DS, Satyanarayana C, Rajagopalan R (2003). Andrographolide, a potential cancer therapeutic agent isolated from *Andrographis paniculata*. J. Exp. Ther. Oncol., 3: 147-158.
- Stanslas J, Liew PS, Iftikhar N, Lee CP, Saad S, Lajis N, Robins RA, Loadman P, Bibby MC (2001). Potential of AG in the treatment of breast cancer. Eur. J. Cancer., 37(Suppl 6): 614.
- Strasser A, O'Connor L, Dixit VM (2000). Apoptosis signalling. Annu. Rev. Biochem., 69: 217-245.
- Tan Y, Chiow KH, Huang D, Wong SH (2010). Andrographolide regulates epidermal growth factor trafficking in epidermoid carcinoma (A-431) cells. Br. J. Pharmacol., 159(7): 1497-1510.
- Vermes I, Haanen C, Reutelingsperger C (2000). Flow cytometry of apoptotic cell death. J. Immunol. Methods., 243: 167-190.
- Yi X, Yin XM, Dong Z (2003). Inhibition of Bid-induced apoptosis by Bcl-2. tBid insertion, Bax translocation, and Bax/Bak oligomerization suppressed. J. Biol. Chem., 278: 16992-16999.
- Zhou J, Zhang S, Ong CN, Shen HM (2006). Critical role of pro-apoptotic Bcl-2 family members in Andrographolide-induced apoptosis in human cancer cells. Biochem. Pharmacol., 72: 132-144.